JOURNAL OF MATERIALS SCIENCE 21 (1986) 3952–3956

A quantitative analysis of hydriding kinetics of magnesium in a Mg/Mg_2Cu eutectic alloy

JAI-YOUNG LEE, H. H. PARK, J. S. HAN
Department of Materials Science and Engineering, Korea Advanced Institute of Science and Technology, PO Box 150 Cheongryang, Seoul, Korea

Comparing the hydriding kinetic equations of magnesium derived from a theoretical model with the experiemental data published by Karty *et al.* [1], the kinetic mechanism of the hydriding reaction of magnesium in a Mg/Mg_2Cu eutectic alloy is analysed. As the eutectic structure of the alloy has the uniform interlamellar spacing of 1 μm, one-dimensional growth of the hydride phase is assumed for the Mg_2Cu-catalysed magnesium. The concurrent hydriding reactions of the vapour-deposited pure magnesium as well as Mg_2Cu-catalysed magnesium are discussed. In both cases, the diffusion of hydrogen through the hydride phase is the rate-controlling step. Quantitative equations for the reaction and the effective particle size of pure magnesium are given, which can be used for reactor design.

1. Introduction

Magnesium has a very high hydrogen storing capacity per unit weight, which is particularly attractive for automobile application as hydrogen fuel. However, magnesium exhibits a very slow hydrogen absorption and desorption reaction rate. To improve the kinetics, many researchers have modified the metal by alloying with various alloying elements [1–9] and by surface coating techniques [10, 11]. For alloy design, the knowledge of accurate hydriding reaction mechanism of pure magnesium is needed. But to obtain intrinsic kinetic data of pure magnesium is very difficult. The reason is that there is always surface contamination and this contaminant layer inhibits hydriding and dehydriding reactions that may affect the chemisorption site of a particle or the layer could be a diffusion barrier. In the latter case the transfer of hydrogen across the contaminant layer could be rate-limiting step. Dymova *et al.* [12] successfully carried out a hydriding reaction of unalloyed magnesium by concurrent ball-milling. The ball-milling cracked the MgO surface layer exposing fresh magnesium surfaces, but during the hydriding reaction some could be contaminated. Stander [13] was also successful using very pure H_2 gas pregettered by magnesium. However in this case about 50% of the magnesium was contaminated.

Recently Karty *et al.* [1] obtained kinetic data of the hydriding reaction of unalloyed magnesium in the Mg/Mg_2Cu eutectic system under the conditions that only pure magnesium can be hydrided. In this system the Mg-vapour deposit formed because of the temperature gradient in the sample container, or as a consequence of the heating and cooling system. They have assumed that the amount of the vapour-deposited magnesium was saturated and obtained the kinetic data at 300 and 400° C with the following relation for the total reaction fraction (F)

$$F = (1 - \varrho)F_1 + \varrho F_2 \quad (1)$$

where F_1 is the reacted fraction of magnesium which is catalysed by Mg_2Cu; F_2 is the reacted fraction of vapour-deposited magnesium; $1-\varrho$ is the fraction of magnesium which is catalysed by Mg_2Cu; and ϱ is the fraction of the saturated amount of the vapour-deposited magnesium which is almost 0.3 ± 0.05 [1].

The Johnson–Mehl–Avrami equation [14] which is the classical rate equation for the nucleation and growth process was adapted to analyse the change of F with time and they concluded the rate-controlling step of the hydriding reaction is the hydrogen diffusion through the hydride phase and Mg_2Cu acts only as a catalyser in the applied hydrogen pressure.

In this work, it is attempted to analyse the kinetic data further in detail with the suggested model. The structural model which has Mg/Mg_2Cu eutectic alloy with the 1 μm interlamellar spacing is derived as shown in Fig. 1. In this structure the hydrogen moves fast through the Mg_2Cu compound or the interface of Mg/Mg_2Cu. Then a hydride film is formed at the interface of Mg/Mg_2Cu and grows as a one-dimensional layer in the magnesium matrix. Simultaneously a hydride layer is also formed at the magnesium vapour deposit. The magnesium vapour deposit contains many surface cracks which are made during the hydriding–dehydriding cycles and seems to be a sponge-like material. As suggested by Mintz *et al.* [2], this material is considered in the concept of the effective particle size. The effective particle size means a unit size less than original particle because of cracks. The shape of vapour-deposited magnesium is assumed to be flat plate in view of the shape of reactor and the amount of sample. Therefore it is also assumed the one-dimensional hydride layer growth from the surface of the flat plate. The kinetic data will be compared with the model. Understanding of all these variables can be used as important data for reactor design.

2. Theory

The hydriding reaction of metal with continuous moving boundary is divided into all possible sequential

0022–2461/86 $03.00 + .12

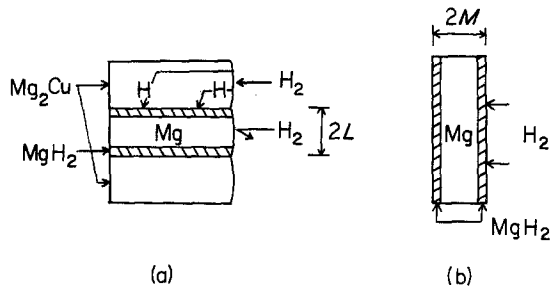

Figure 1 Model of hydriding of Mg_2Cu-catalysed magnesium and hydriding of vapour-deposited pure magnesium.

reaction steps and when one of them is rate controlling, overall rate equation is derived.

2.1. Mg_2Cu-catalysed magnesium

In Fig. 1a as the surface of magnesium is contaminated with oxides, the hydrogen may transfer mainly through the Mg_2Cu phase or Mg_2Cu/Mg interface. The hydrogen diffusion through Mg_2Cu phase which acts as catalyser [1] or through Mg_2Cu/Mg interface should be fast, this step can be ignored as a rate-controlling one. The possible rate-controlling steps for the hydriding reaction will be as follows: (a) the mass transfer of hydrogen molecules to the metal surface; (b) the hydrogen diffusion in the hydride phase; and (c) the interfacial chemical reaction between hydride and magnesium.

2.2. Vapour-deposited pure magnesium

Because the vapour-deposited magnesium is formed under high purity hydrogen atmosphere, the surface of the magnesium should be clean and hydrogen is easily absorbed through the surface. Therefore possible rate-controlling steps are: (a) the mass transfer of hydrogen molecules to the metal surface; (b) the chemisorption of hydrogen molecules on the surface of the specimen; (c) the hydrogen diffusion through the hydride phase; and (d) the interface chemical reaction between metal and hydride.

2.3. Theoretical rate equations

Park and Lee [15] had derived rate equations applying spherical moving boundary model for the $LaNi_5$ system to explain the hydriding kinetic mechanism. However in this study the hydriding reaction equations of the flat plate for one-dimensional growth are derived as follows.

As the hydriding reaction rate R, is a function of temperature, pressure and reacted fraction, R can be described as Equation 2

$$R = Kf(T)f(P)f(F) \tag{2}$$

where: K is the rate constant; T is the temperature; P is the pressure; and F is the reacted fraction.

Rudman and co-workers used the pressure sweep method [1, 16–18] to obtain the kinetic data at a constant pressure and temperature. The method is described in [16] in detail. Therefore R is reduced to Equation 3

$$R = K'f(F) \tag{3}$$

where K' is the rate constant at constant T and P.

Now the reaction rate equation of each step is only a function of the reacted fraction F, which varies with time t. The overall rate equations when each step is rate controlling are expressed in F against t plot as follows:

2.3.1. The mass transfer of hydrogen molecules to the metal surface

If the mass transfer in the system is rate-controlling step. Two types of gas flow, forced and Knudsen flow, should be considered by comparing the gas mean free path (λ) and diameter of cracks ($2r$). For the case of forced flow ($\lambda < 2r$), the reaction rate equation [15] is

$$F = \frac{Ar^2(P_0^2 - P_{eq}^2)}{16RT\eta\Delta L} \tag{4}$$

where: A is the crack surface area; P_0 is the applied pressure; P_{eq} is the equilibrium hydrogen pressure for the hydride formation at T; T is the reaction temperature; R is the gas constant; η is the viscosity of hydrogen gas; and ΔL is the channel length of gas flow.

For the case of Knudsen flow ($\lambda > 2r$), the rate equation is

$$F = \frac{AD_k(P_0 - P_{eq})}{RT\Delta L} \tag{5}$$

where: D_k is the Knudsen diffusion coeffcient and $(2r/3)/(8RT/2M)^{1/2}$; and M is the molecular weight of hydrogen.

2.3.2. The chemisorption of hydrogen on the metal surface

The rate equation when chemisorption of hydrogen on the metal surface is rate controlling is [15] given by

$$F = k_2(P_0 - P_{eq})t \tag{6}$$

where: k_2 is the rate constant.

2.3.3. The hydrogen diffusion in hydride

The hydrogen diffusion through the hydride phase being rate-controlling step. The rate equation of the flat plate for one-dimensional growth can be derived, based on the continuous moving boundary model [19], as Equation 7

$$F = \left(\frac{2D_H\Delta C_H}{\varrho_H L^2}\right)^{1/2} t^{1/2} \tag{7}$$

where: D_H is the diffusivity of hydrogen in the hydride phase; ΔC_H is the concentration difference between hydride phase and the hydrogen equilibrium concentration; ϱ_H is the hydrogen concentration in hydride phase; and L is the distance in that direction hydride phase in growing.

2.3.4. The interfacial chemical reaction between metal and hydride

If the chemical reaction between metal phase and the hydride phase is the rate-controlling step, the rate equation can be derived as follows

$$F = \frac{K_s C_H}{L\varrho_H} t \tag{8}$$

where: K_s is the rate constant for metal/hydride inter-

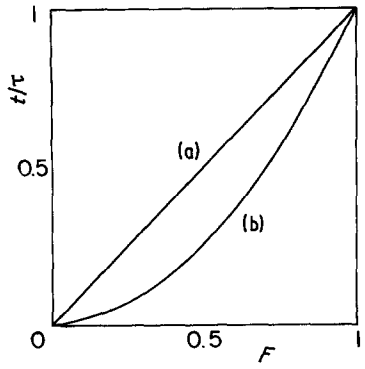

Figure 2 Schematic diagrams of t/τ against reacted fraction (a) gas phase mass transfer, chemisorption of H_2 on the sample surface, chemical reaction at the interface, (b) diffusion through hydride phase.

face reaction; and C_H is the hydrogen concentration at the interface.

3. Results and discussion

With the reaction rate equations established above, schematic diagrams are plotted in Figs 2 and 3 by F against t and R against F, respectively. Fig. 2 shows a relation of F against t/τ (τ is the time required to complete the reaction). When mass transfer, chemisorption or chemical reaction is the rate-controlling step, the relation is linear like curve (a). Diffusion in the hydride phase being the rate-controlling step, the relation is concave downward, curve (b). Fig. 3 shows a schematic relation of the R against F plot. The linear curve (a) is for the case of mass transfer, chemisorption and chemical reaction being rate controlling and curve (b) for the case of diffusion, namely the further the reaction proceeds the slower kinetics are. Figs 4 and 5 show hydriding kinetics at constant pressure which were derived from the pressure sweep data [1]. Comparing the shape of curves of Figs 4 and 5 with Fig. 2, the hydriding reaction of magnesium at 300 and 400° C is controlled by the hydrogen diffusion through the hydrogen phase.

The relations of rate against reacted fraction are shown at 300, 400° C in Figs 6 and 7, respectively. As the reaction temperature is increased, reaction rate is increased and as the reacted fraction is increased, the

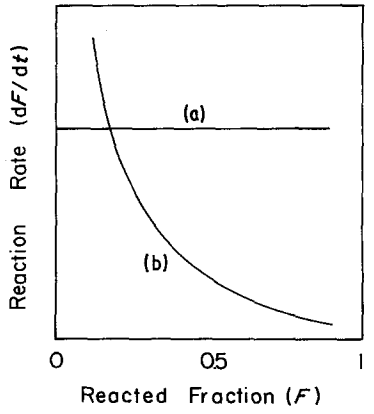

Figure 3 Schematic diagram of various type hydrogen absorption rate depending on reacted fraction. (a) mass transfer, chemisorption and chemical reaction, (b) hydrogen diffusion in the hydride phase.

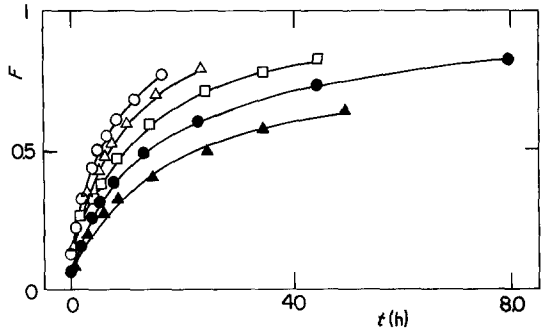

Figure 4 Hydriding kinetics of magnesium at constant pressure at 300° C. (○) 4.76; (△) 4.42; (□) 3.74; (●) 3.06; (▲) 2.38 atm.

reaction rate is decreased. Comparing the shape of curves in Figs 6 and 7 with Fig. 3, the rate controlling step of hydriding of magnesium is also hydrogen diffusion through the hydride phase.

To investigate hydriding behaviour with the size of the Mg_2Cu-catalysed magnesium and the vapour-deposited pure magnesium. Let the Mg_2Cu-catalysed magensium (Fig. 1a) be system 1 and the vapour-deposited pure magnesium (Fig. 1b) be system 2. And let the distance through which the hydriding reaction proceeds be L for system 1 and M for system 2, because the reaction starts from both sides of plate shaped magnesium. According to Rudman's observation [1], L is about 0.5 μm. The effective particle size is about 1 μm for system 1. It is assumed that the effective particle size of system 1 is constant ($2L \doteqdot 1\mu$m) throughout the whole hydriding–dehydriding reactions. But considering the sintering effect of the metal [20], the average effective particle size of system 2 at 300 and 400° C has a relation of $2M_{300} < 2M_{400}$. Because of size difference of system 1 and 2 they may not finish the reaction simultaneously. To analyse the hydriding behaviour a few relations between L and M are classified as follows:

1. $L > M$

In this case, system 2 finishes the hydriding reaction faster than system 1. If it takes time, t_2 to complete whole reaction and at time t_1 ($t_1 < t_2$) system 2 finishes the reaction, only system 1 will continue the reaction after t_1. Therefore at $0 \leqslant t \leqslant t_1$ the total reacted fraction F is a function of time of system 1 and 2 and at $t_1 < t < t_2$ F is a function of time of only system 1. For the above 2 cases, the relation, F against t combining

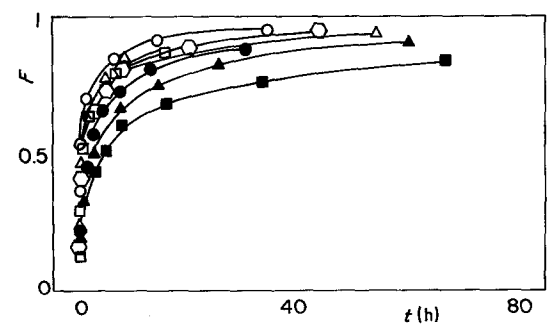

Figure 5 Hydriding kinetics of magnesium at constant pressure at 400° C. (○) 18.03; (△) 17.68; (□) 17.35; (⬡) 17.01; (●) 16.67; (▲) 16.63; (■) 15.99 atm.

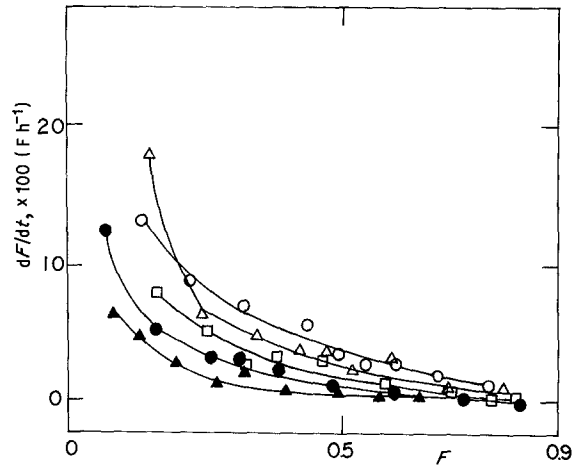

Figure 6 Hydrogen absorption rate with reacted fractions and hydrogen pressures at 300° C. (○) 4.76; (△) 4.42; (□) 3.74; (●) 3.06; (▲) 2.38 atm.

Equations 1 and 7 results in Equations 9 and 10 $0 \leqslant t \leqslant t_1$ (simultaneous reaction of system 1 and 2)

$$F = \varrho\left(\frac{2D_H\Delta C_H}{\varrho_H M^2}\right)^{1/2} t^{1/2} + (1-\varrho)\left(\frac{2D_H\Delta C_H}{\varrho_H L^2}\right)^{1/2} t^{1/2} \tag{9}$$

$t_1 < t \leqslant t_2$ (reaction of only system 1)

$$F = \varrho + (1-\varrho)\left(\frac{2D_H\Delta C_H}{\varrho_H L^2}\right)^{1/2} t^{1/2} \tag{10}$$

From Equations 9 and 10 one can expect a linear relation passing the origin in the F against $t^{1/2}$ plot at $0 < t < t_1$ and after t_1 another linear relation with the intersection of F axis at ϱ ($=0.3 \pm 0.05$ [1]).

2. $L \doteqdot M$

In this case both systems finish the hydriding reaction almost simultaneously. The relation of F against t will follow Equation 9.

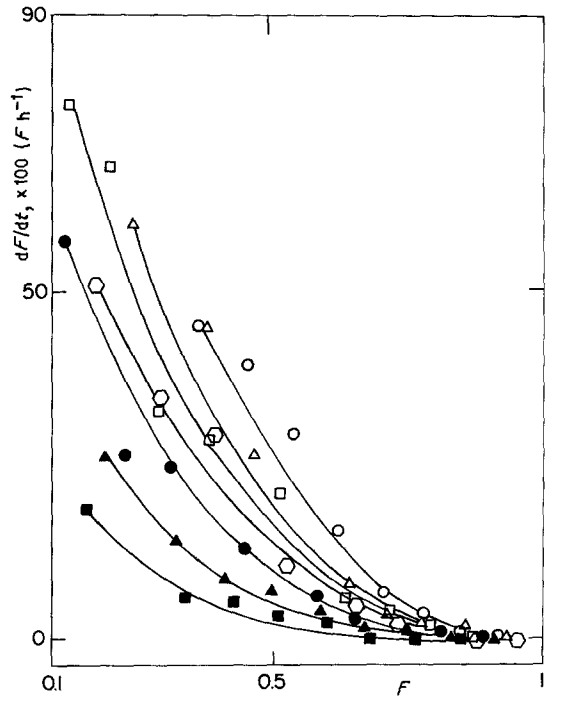

Figure 7 Hydrogen absorption rate with reacted fractions and hydrogen pressures at 400° C. (○) 18.03; (△) 17.68; (□) 17.35; (⬡) 17.01; (●) 16.67; (▲) 16.33; (■) 15.99 atm.

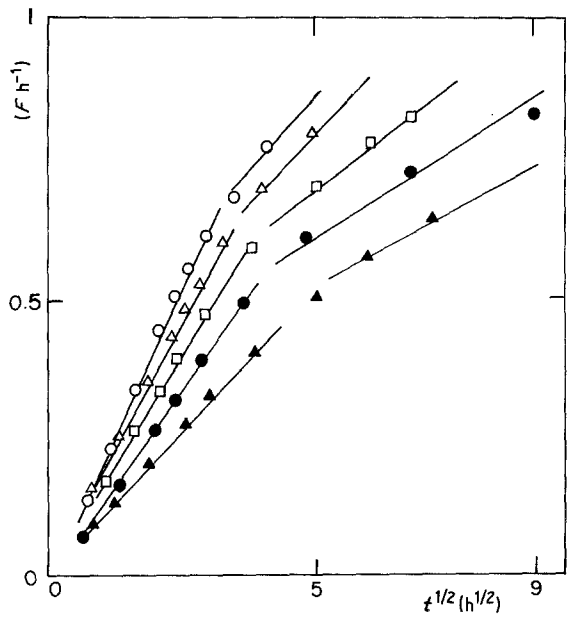

Figure 8 Reacted fraction with reaction time at various hydrogen pressures at 300° C. (○) 4.76; (△) 4.42; (□) 3.74; (●) 3.06; (▲) 2.38 atm.

3. $L < M$

In this case system 1 completes the reaction faster than system 2 (with the time division similar to the case 1). Letting the time which takes to complete whole reaction be t_2' and the time which takes to finish reaction for system 1 be t_1', and combining Equations 1 and 7, Equations 11 and 12 can be derived. $0 \leqslant t \leqslant t_1'$ (simultaneous reaction of system 1 and 2)

$$F = \varrho\left(\frac{2D_H\Delta C_H}{\varrho_H M^2}\right)^{1/2} t^{1/2} + (1-\varrho)\left(\frac{2D_H\Delta C_H}{\varrho_H L^2}\right)^{1/2} t^{1/2} \tag{11}$$

$t_1' < t \leqslant t_2'$ (reaction of only system 2)

$$F = (1-\varrho) + \varrho\left(\frac{2D_H\Delta C_H}{\varrho_H M^2}\right)^{1/2} t^{1/2} \tag{12}$$

From the above relations, in the time span of $0 \leqslant t \leqslant t_1'$ the F against $t^{1/2}$ plot is a straight line passing through the origin and after t_1' another straight line which passes an intersection of F axis, $1-\varrho$ ($=0.7 \pm 0.05$ [1]), will continue.

To identify which case is the real situation Rudman's data was reanalysed and plotted by F against $t^{1/2}$ at 300 and 400° C in Figs 8 and 9. Fig. 8 shows initially all the plots pass through origin and then the slope of the straight line deviate to have intersections of the F axis. The values of intersection are about 0.3 ± 0.05. Both the change of slope and the value of the intersection correspond to case 1 ($L \geqslant M_{300}$) in the above analysis. The M value is calculated by the ratio of slopes of two curves of Equations 9 and 10

$$\frac{\text{slope } (0 \leqslant t < t_1)}{\text{slope } (t_1 < t < t_2)} = \frac{\varrho L + (1-\varrho)M}{M(1-\varrho)} \tag{13}$$

with $\varrho = 0.3 \pm 0.05$, $L = 0.5\,\mu$m and the slope ratio of about 2 from Fig. 8. The M_{300} value is $0.17 \sim 0.27\,\mu$m. The average effective particle size, $2M_{300}$, of

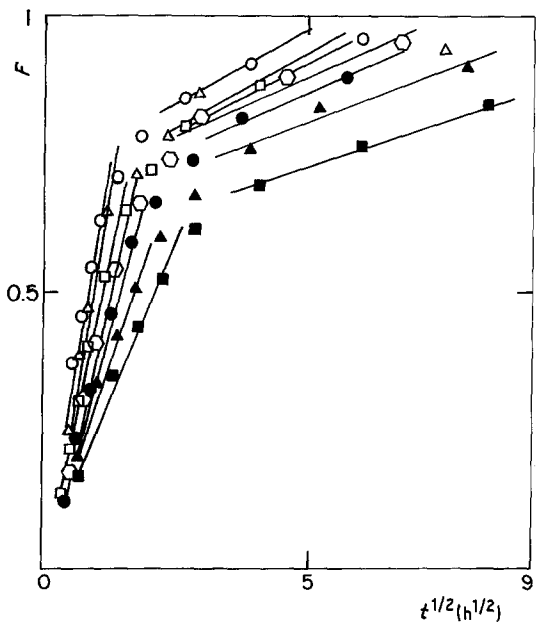

Figure 9 Reacted fraction with reaction time at various hydrogen pressures at 400° C. (○) 18.03; (△) 17.68; (□) 17.35; (⬡) 17.01; (●) 16.67; (▲) 16.63; (■) 15.99 atm.

vapour-deposited magnesium is 0.34 ~ 0.56 μm. Fig. 9 shows almost the same phenomena except the value of intersection. The values of the intersection are about 0.7 ± 0.05. This case corresponds to the case 3 ($L < M$). M_{400} is calculated to be 1.3 ~ 2.1 μm. The average effective particle size of vapour-deposited magnesium at 400° C is 2.6 ~ 4.2 μm.

4. Conclusions

The hydriding reactions of magnesium in a Mg/Mg_2Cu eutectic alloy is well explained by the one-dimensional continuous moving boundary model. The both hydriding reactions of magnesium in a eutectic alloy and that of the vapour-deposited pure magnesium are controlled by the hydrogen diffusion in the hydride phase. As the average particle size of Mg/Mg_2Cu eutectic alloy is 1 μm, the effective particle size of vapour-deposited pure magnesium at 300° C is in the range of 0.34–0.54 μm. And the reaction equations for each step of hydriding reactions are

$0 \leqslant t \leqslant t_1$

$$F = \varrho\left(\frac{2D_H\Delta C_H}{\varrho_H M^2}\right)^{1/2} t^{1/2} + (1-\varrho)\left(\frac{2D_H\Delta C_H}{\varrho_H L^2}\right)^{1/2} t^{1/2} \quad (14)$$

$t_1 < t \leqslant t_2$

$$F = \varrho + (1-\varrho)\left(\frac{2D_H\Delta C_H}{\varrho_H L^2}\right)^{1/2} t^{1/2} \quad (15)$$

The average effective particle size of the vapour-deposited pure magnesium at 400° C is calculated to be 2.6 ~ 4.2 μm. And the corresponding rate equations are

$0 \leqslant t \leqslant t_1'$

$$F = \varrho\left(\frac{2D_H\Delta C_H}{\varrho_H M^2}\right)^{1/2} t^{1/2} + (1-\varrho)\left(\frac{2D_H\Delta C_H}{\varrho_H L^2}\right)^{1/2} t^{1/2} \quad (16)$$

$t_1' < t \leqslant t_2'$

$$F = (1-\varrho) + \varrho\left(\frac{2D_H\Delta C_H}{\varrho_H M^2}\right)^{1/2} t^{1/2} \quad (17)$$

The above data can be utilized for reactor design.

References

1. A. KARTY, J. G. GENOSSAR and P. S. RUDMAN, *J. Appl. Phys.* **50** (1979) 7200.
2. M. H. MINTZ, Z. GAVRA and Z. HADARI, *J. Inorg. Nucl. Chem.* **40** (1978) 765.
3. D. L. DOUGLAS, *Metall. Trans. A* **6A** (1975) 2179.
4. E. AKIBA, K. NORMURA and S. ONO, *J. Less Common Metals* **89** (1983) 145.
5. B. VIGEHOLM, J. KJOLLER, B. LARSEN and A. S. PEDERSEN, *ibid.* **89** (1983) 135.
6. D. L. DOUGLAS, in Proceedings of an International Symposium held in Gelio, Norway, 14-19, August 1977 (Pergamon Press, New York) pp. 151–184.
7. M. H. MINTZ, S. MALKIELY, Z. GAVRA and Z. HADARI, *J. Inorg. Nucl. Chem.* **40** (1978) 1949.
8. P. S. RUDMANN, *J. Appl. Phys.* **50** (1979) 7195.
9. F. G. EISENBERG, D. A. ZAGNOLI and J. J. SHERIDAN III, *J. Less Common Metals* **74** (1980) 323.
10. H. IMAMURA, M. KAWAHIGASHI and S. TSUCHIYA, *ibid.* **95** (1983) 157.
11. F. G. EISENBERG, D. A. ZAGNOLI and J. J. SHERIDAN III, *ibid.* **74** (1980) 323.
12. T. N. DYMOVA, Z. K. STEVLYADKINA and V. G. SAFRONOV, *Russ. J. Inorg. Chem.* **6** (1961) 389.
13. C. M. STANDER, *Z. Physik, Chem.* **104** (1977) 229.
14. W. A. JOHNSON and R. F. MEHL, *Trans. AIME* **135** (1939) 416.
15. C. N. PARK and J. Y. LEE, *J. Less Common Metals* **83** (1982) 39.
16. J. Y. LEE, S. M. BYUN, C. N. PARK and J. K. PARK, *ibid.* **87** (1982) 149.
17. J. Y. LEE, C. N. PARK and S. M. BYUN, *ibid.* **89** (1983) 163.
18. J. Y. LEE and S. H. LIM, *ibid.* **97** (1984) 59.
19. O. LEVENSPIEL, in "Chemical Reaction Engineering" (Wiley, New York, 1962) Ch. 12.
20. B. VIGEHOLM, J. KJOLLER and B. LARSEN, *J. Less Common Metals* **74** (1980) 341.

Received 4 October 1985
and accepted 21 January 1986